frontiers in Materials

ORIGINAL RESEARCH
published: 05 June 2020
doi: 10.3389/fmats.2020.00141

Structure Characterization and Biodegradation Rate of Poly(ε-caprolactone)/Starch Blends

*Martina Nevoralová[1], Marek Koutný[2], Aleksandra Ujčić[1], Zdeněk Starý[1], Jana Šerá[2], Helena Vlková[1], Miroslav Šlouf[1], Ivan Fortelný[1] and Zdeněk Kruliš[1]**

[1] Institute of Macromolecular Chemistry, Czech Academy of Sciences, Prague, Czechia, [2] Faculty of Technology, Tomas Bata University in Zlín, Zlín, Czechia

The present paper focuses on the effects of blending poly (ε-caprolactone) (PCL) with thermoplastic starch (TPS) on the final biodegradation rate of PCL/TPS blends, emphasizing the type of environment in which biodegradation takes place. The blends were prepared by melt-mixing the components before a two-step processing procedure, which strongly affects the degree of plasticization and therefore the final material morphology, as was detailed in the previous work, was used for the thermoplastic starch. The concentration row of pure PCL over PCL/TPS blends to pure TPS was analyzed for biodegradation in two different environments (compost and soil), as well as from a morphological, thermomechanical, rheological, and mechanical point of view. The morphology of all the samples was studied before and after biodegradation. The biodegradation rate of the materials was expressed as the percentage of carbon mineralization, and significant changes, especially after exposure in soil, were recorded. The crystallinity of the measured samples indicated that the addition of thermoplastic starch has a negligible effect on PCL-crystallization. The blend with 70% of TPS and a co-continuous morphology demonstrated very fast biodegradation, with the initial rate almost identical to pure TPS in both environments while the 30% TPS blend exhibited particle morphology of the starch phase in the PCL matrix, which probably resulted in a dominant effect of the matrix on the biodegradation course. Moreover, some molecular interaction between PCL and TPS, as well as differences in flow and mechanical behavior of the blends, was determined.

Keywords: poly (ε-caprolactone), thermoplastic starch, biodegradation rate, soil, morphology

OPEN ACCESS

Edited by:
Guilherme Mariz de Oliveira Barra, Federal University of Santa Catarina, Brazil

Reviewed by:
Fabrizio Sarasini, Sapienza University of Rome, Italy
Jorge Gracida, Universidad Autónoma de Querétaro, Mexico
Larissa Nardini Carli, Federal University of Santa Catarina, Brazil

****Correspondence:***
Zdeněk Kruliš
krulis@imc.cas.cz

Specialty section:
This article was submitted to Polymeric and Composite Materials, a section of the journal Frontiers in Materials

Received: *26 July 2019*
Accepted: *24 April 2020*
Published: *05 June 2020*

Citation:
Nevoralová M, Koutný M, Ujčić A, Starý Z, Šerá J, Vlková H, Šlouf M, Fortelný I and Kruliš Z (2020) Structure Characterization and Biodegradation Rate of Poly(ε-caprolactone)/Starch Blends. Front. Mater. 7:141. doi: 10.3389/fmats.2020.00141

INTRODUCTION

The biodegradation rate of polymeric materials is a crucial issue becoming more important due to increasing environmental concerns (Swain et al., 2004; Jayasekara et al., 2005; Rochman et al., 2013; Narancic et al., 2018). One of the solutions to the problem is the development and usage of materials made of biodegradable polymers like poly (ε-caprolactone) (PCL) (Funabashi et al., 2009), starch, and others. PCL is a hydrophobic and partially crystalline aliphatic polyester with excellent deformability (Singh et al., 2003; Imre and Pukánszky, 2013; Rudnik, 2013), but some of its characteristics, e.g., low melting temperature ($T_m \sim 60^\circ C$) (Funabashi et al., 2009; Düskünkorur, 2012) or relatively low strength, prevent a broader application of this polymer, which is at present

very popular, e.g., for biomedical or tissue applications (Singh et al., 2003; Leja and Lewandowicz, 2010; Chang et al., 2017). The use of PCL materials in the food-packaging industry and agriculture is very advantageous due to their resistance to water and oil, non-toxicity, and biodegradability (Funabashi et al., 2009; Rudnik, 2013). Therefore, many attempts have been made to combine PCL with other polymers to modify its properties and degradation in the environment (Bastioli, 1998; Averous et al., 2000; Wang et al., 2003; Campos et al., 2012; Mittal et al., 2015; Ostafinska et al., 2015).

A parallel interest in the field of developing new and especially inexpensive and biodegradable materials has led to a substantive amount of research in polymer blends containing starch (Wang et al., 1995; Averous et al., 2000; Avérous, 2004). Starch is a mixture of amylose and amylopectin (Sessini et al., 2018). In order to obtain a homogeneous thermoplastic material, native starch must be plasticized to disrupt the starch grains and reduce the amount of intramolecular and intermolecular hydrogen bonds. Thermoplastic starch (TPS) is generally prepared by gelatinization of native starch (Avérous, 2004) in the presence of an appropriate plasticizer under the influence of heat and shear (Wang et al., 2003; Parulekar and Mohanty, 2007). Thermoplastic materials based on starches can be prepared by solution casting, melt mixing, or the combination of both methods, which was described in detail in our previous work (Ostafińska et al., 2017a). Unfortunately, the application of materials based on thermoplastic starches is still limited because of their poor water resistance and low mechanical strength (Wang et al., 2003).

For the reasons mentioned above, PCL/TPS blends seem to be interesting and promising low-cost biodegradable materials with tailored properties, and have thus recently been extensively investigated (Avérous, 2004; Rudnik, 2013; Villar et al., 2017). The final properties of immiscible polymer blends depend directly on their morphology, which is affected particularly by blend composition and interfacial tension, but also by rheological properties of blend components and processing conditions (Horák et al., 2005; Imre and Pukánszky, 2013). Depending on the origin of native starch, and thus on the amylose and amylopectin content, the viscosity and elasticity of the plasticized materials can vary substantially (Huneault and Li, 2012; Nevoralová et al., 2019). Due to immiscibility of PCL and starch (Shaw, 1985), PCL/TPS blends exhibit heterogeneous phase structure (Imre and Pukánszky, 2013). Therefore, it is obvious that the optimization of the rheological properties of any immiscible polymer blend including PCL/TPS and the resulting morphologies is essential to obtain materials with balanced end-use properties tailored to specific application (Fortelný et al., 2008). Nevertheless, to the best of our knowledge, both the rheological behavior and the morphology of starch-based biodegradable polymer blends have not been discussed in detail.

Depending on the morphology and surrounding conditions, each polymer degrades at least to some extent. Generally, polymers can be described as degradable when degradation leads to a reduction in molecular weight by chain scission of the main chain on a certain time scale depending on environmental conditions and on whether the final products are of low molecular weight. In biodegradable polymers, the cleavage of the chain is often caused by enzymatic processes that are usually accompanied and supported by physicochemical phenomena leading to a complete degradation of the polymer (Imre and Pukánszky, 2013). According to several authors (Wang et al., 2003; Khatiwala et al., 2008; Mudhoo et al., 2011), PCL, as a member of the aliphatic polyesters group, is a material susceptible to microbial degradation. According to Bastioli, a product can be claimed as biodegradable even though the PCL homopolymer biodegradation rate is very low (Bastioli, 1998). The biodegradation of PCL involves a simple hydrolysis of ester bonds and/or an enzymatic attack (Albertsson and Varma, 2002; Rutkowska et al., 2002; Düskünkorur, 2012). The biodegradability of PCL was observed in the presence of microorganisms in diverse environments, including river and lake waters, sewage sludge, farm soil, paddy soil, creek sediment, roadside sediment, pond sediment, and compost (Rutkowska et al., 2002; Khatiwala et al., 2008; Leja and Lewandowicz, 2010). During the degradation process in a biotic environment, the amorphous fraction of PCL degrades before the crystalline fraction (Leja and Lewandowicz, 2010).

According to literature, PCL can be biodegraded within a period ranging from a few months to several years depending on its molecular weight, degree of crystallinity, morphology, porosity, sample thickness, and the surrounding environment (Labet and Thielemans, 2009; Leja and Lewandowicz, 2010). It is assumed that the low melting point of PCL should be favorable for composting as a means of disposal, because the temperature obtained during composting is usually around or above PCL melting temperature (60°C). Sánchez et al. mentioned that thermophilic composting is one of the promising technologies for transforming biodegradable plastics into fertilizers (Sanchez et al., 2000). Jayasekara and co-workers reported that molar mass and crystallinity are the main factors affecting biodegradability (Jayasekara et al., 2005). Furthermore, it has been reported that the presence of polysaccharides in the case of mixtures enhances the biodegradation rate of PCL (Vroman et al., 2009; Düskünkorur, 2012). Many authors have also pointed out that the degradation of the more readily biodegradable component controls the rate of degradation of polymer blends (Jayasekara et al., 2005; Leja and Lewandowicz, 2010).

From the biodegradation environment point of view there are a lot of studies with inconsistent conclusions. On the one hand, PCL appears to be readily biodegradable under industrial composting conditions defined by ISO 14855. On the other hand, reports on PCL biodegradability in soil reveal a surprising variability of results from fast degradation characterized by a PCL mass loss of 95% in 1 year (Potts et al., 1973) or even about 90% in 5 months (Narancic et al., 2018) to very slow biodegradation of the same material expressed by a mass loss of only 32% after 2 years (Innocenti, 2005). Such an extreme inconsistency is hard to explain, especially since some important details of the material parameters or the soil environment used were not always comprehensively stated in all the studies (Innocenti, 2005). Generally, the molecular weight (M_w) of the polymer appears to play an important role in the PCL biodegradation (Cesur, 2018).

Blends of PCL and starch are assumed to be completely biodegradable because each component of the blends is readily biodegradable (Iwamoto and Tokiwa, 1994; Vikman et al., 1999; Wang et al., 2003; Jayasekara et al., 2005). The rate of degradation of polymer blends is initially controlled by the degradation of the more readily biodegradable component. The initial degradation process interferes with the structural integrity of the polymer and considerably increases the surface area for enzyme attack. The exposure of the remaining polymer to microbes and secreted degradative enzymes is then enhanced (Jayasekara et al., 2005). Increasing the hydrophilicity of the polymers should increase their susceptibility to enzymatic attack, so this should also be seen on the rate of biodegradation of PCL/TPS mixtures depending on the ratio of these components (Jayasekara et al., 2005). Vikman et al. analyzed PCL/TPS samples prepared in the piece form and in the milled form (Vikman et al., 1999). The authors reported that the surface area of the samples was a very important parameter for biodegradation and that the PCL layer on the surface of the blend slowed the biodegradation process. In addition, the degradation of this blend was more rapid at higher blending temperatures, a fact that the authors associated with a coarser phase structure of the blend. Generally, it is often very difficult to compare published results because of different starch types used, as this significantly affects the course of biodegradation experiments, too. Although the topic of PCL blends with TPS has been the center of attention for several years, the effect of their morphology on the rate of biodegradation has not been systematically studied enough.

The aim of this paper is to contribute to a better understanding of the relationships between the composition and the PCL/TPS blend's morphology and following from that their biodegradation rate in two different environments—compost and soil.

EXPERIMENTAL

Materials

The polymers used in this study were commercial polyester—poly(ε-caprolactone) Capa 6800 (PCL) supplied by Perstorp Group (Sweden) in granular form with an average molecular weight of M_w 80,000 g·mol^{-1} and the melting point of 58°C, and wheat starch A "Soltex NP1," provided by Amylon a.s. (Czech Republic). Anhydrous glycerol from Lachner (Czech Republic) with purity > 99% was used as a plasticizer. Hydrochloric acid (HCl) was purchased from Lachner (Czech Republic). Aqueous solutions were prepared using distilled water.

Preparation of Blend Samples

The PCL/TPS-blends and their neat polymer samples were prepared by melt-mixing procedure in micro-extruder DSM (Netherlands).

Thermoplastic starch component of blends was prepared by a two-step process, which was described in detail in our previous work (Ostafińska et al., 2017a). During this procedure, the starch, glycerol (30 wt. %) and distilled water (water/starch = 6/1) were premixed with a magnetic stirrer for 30 min at laboratory temperature and then the mixture was kept in conditions of continuous agitation for another 15 min at elevated temperature (above 65°C) until the viscosity increased significantly. Then the mixture was cast in a Petri dish into a form of about 2-mm-thick film and dried at laboratory temperature (at relative humidity RH = 50–55%) for 2–3 days, followed by 4 days in a desiccator with saturated solution of sodium bromide (RH = 57%) (Ostafinska et al., 2018). In the following step, the thermoplastic starch film was cut into small pieces and after that homogenized by melt-mixing at screw speed of 160 rpm and temperature of 130°C for 8 min. Finally, the TPS-material was compression-molded in a Fontijne Grotnes (Netherlands) hydraulic press at 130°C (2 min at 50 kN and then 1 min at 100 kN) into rectangular specimens with a thickness of 2 mm and 4 mm, which were subsequently cooled down to laboratory temperature for 15 min.

The blends were prepared by the melt-mixing of PCL (dried in vacuum oven at 40°C for 12 h) together with homogenized TPS at the same conditions as those of homogenization TPS-procedure in the respective weight ratio of the individual blend's components (PCL/TPS 70/30, 50/50, and 30/70). Due to a relative low melting point of PCL, the blending temperature of neat PCL was set to 120°C.

Methods of Characterization

Differential Scanning Calorimetry

Differential scanning calorimetry (DSC) analysis was carried out in a TA Instruments Q2000 calorimeter with nitrogen as purge gas (50 cm^3 min^{-1}). The instrument was calibrated using indium as a standard. Samples of ∼10 mg were encapsulated into aluminum hermetic pans. The analysis was performed in a heating–cooling–heating from −90 to 150°C cycle at a constant heating rate of 10°C·min^{-1}. The crystallinity degree (X_c) of samples was calculated by the following equation (1):

$$X_c = \frac{H_m}{W \times H_m^0} \times 100 \quad (1)$$

where H_m is the experimental fusion enthalpy [Jg^{-1}], H_m^0 is the fusion enthalpy of 100% crystalline PCL, which is, according to Nagata and Yamamoto (2009), equal to 135 Jg^{-1}, and W is the weight fraction of PCL in the sample. The values presented in the paper are average values from two independent measurements. Therefore, no standard deviations were evaluated. Generally, the reproducibility of these measurements was very good, and the values did not differ by more than 5%.

Scanning Electron Microscopy

The phase structure morphology of the PCL/TPS blends and homogeneity of their pure components were observed with a scanning electron microscope (SEM) Quanta 200 FEG (FEI, Czech Republic) using secondary electron imaging at 10 kV. Before the observation in the SEM, the samples were fractured in liquid nitrogen, then the fractured surface was smoothed, and the TPS-phase of cryo-fractured surface of all blends was etched out in 6 N HCl solution for 10 min. The prepared samples were fixed on a metallic support with a conductive silver paste (Leitsilber G302; Christine Groepl, Austria) and finally sputtered with ∼4-nm-thin platinum layer by means of a vacuum sputter coater

SCD 050 (Balzers, Liechtenstein) in order to prevent charging and minimize sample damage due to the electron beam.

Rheological Characterization

Rheological behavior of the investigated materials was studied using a rotational rheometer Physica MCR 501 (Anton Paar GmbH, Austria) equipped with a convection temperature device (CTD 450) in dynamic mode. To minimize the water evaporation effect before the measurement, all the samples were stored in a desiccator. The basic rheological characteristics of PCL/TPS blends and their neat components were examined in oscillatory shear flow using parallel-plate geometry with a plate diameter of 25 mm. Frequency sweep experiments were performed in the frequency range from 10^{-1} to 10^{2} rad/s at strain amplitude of 0.05% and constant temperature of 120°C. Linear viscoelasticity region was determined by dependence of the storage modulus on strain amplitude of deformation at constant frequency of 1 Hz. The thermal stability of the materials during rheological measurements was confirmed by time sweeps experiments at 120°C. To ensure uniform temperature field all samples were equilibrated for 2 min prior to the measurements start.

Thermo-Mechanical Characterization

The thermo-mechanical characterization of investigated PCL/TPS blends and neat components was tested by dynamic mechanical thermal analysis (DMTA) in rectangular torsion geometry using the same rheometer used for their basic rheological characterization. Temperature sweeps were carried out in the temperature range from −80 to 150°C with the heating rate of 3°C min^{-1} at constant frequency of 1 Hz and strain of 0.05% set on the base of an amplitude sweep. The results of the three specimens of each material were averaged.

Micro-Indentation Hardness Testing

Micromechanical properties of the samples were characterized by means of instrumented micro-indentation hardness testing (Micro-Combi Tester, CSM Instruments, Switzerland). Smooth surfaces for micro-indentation testing were prepared from compression molded plates (thickness 2 mm), which were also used for the above-described rheological and DMA measurements. The plates were cut perpendicularly with a rotary microtome (RM 2255; Leica, Austria) using a freshly broken glass knife (Glass Knife Maker EM KMR3; Leica, Austria). For each sample, at least two independent cut surfaces were prepared and at least 15 indentations were performed on each surface. Therefore, each micromechanical property represents an average of at least 30 independent measurements. The indentations were performed with a diamond square pyramid with geometry according to Vickers (angle between two non-adjacent phases 136°). The indenter was forced against the polymer surface with the following parameters: maximum load $F = 50$ gf (490.5 mN), dwell time (time of maximal load) $t = 60$ s, and fast linear loading and unloading rate 24,000 mN/min (400 mN/s). For given experimental conditions, the average size of the imprints was $>100\,\mu m$, which was higher than the average size phase domains in all studied systems. Consequently, the micro-indentation results represented the whole system and could be compared with macroscopic properties. Final F-h curves (where F is the loading force and h is the penetration depth) were employed in the calculation of four micromechanical properties: indentation hardness (H_{IT}), indentation modulus (E_{IT}), indentation creep (C_{IT}), and the elastic part of the indentation work (η_{IT}). All calculations were performed within the original software coming with the indenter (Indentation 5.18, CSM Instruments, Switzerland), according to the theory of Oliver and Pharr (1992); the details about the calculation of C_{IT} and η_{IT} were described elsewhere (Herrman, 2011; Slouf et al., 2018).

Biodegradation Tests

Biodegradation Under Composting Conditions

The method utilized was based on a previously published protocol by Dřímal et al. (2007) with some modifications. Biodegradation tests were performed in 500 ml biometric flasks equipped with septa mounted on stoppers. Three components were weighed into the flasks: polymer film samples cut into 2 mm pieces (100 mg), mature compost (2.5 g of dry weight) and perlite (5 g). Sample flasks were incubated at 58°C. Head space gas was sampled at appropriate intervals through the septum with a gas-tight needle and conducted through a capillary into the gas analyzer (UAG, Stanford Instruments, USA) to determine the concentration of CO_2. From the CO_2 concentration found, the percentage of mineralization relative to the carbon content of the sample was calculated. The endogenous production of the CO_2 by compost in blank incubations was always subtracted to obtain values representing net sample mineralization.

Biodegradation in Soil Condition

The laboratory procedure used was based on ISO 17556 but was miniaturized and adapted for small laboratory samples of materials. Biodegradation tests (Stloukal et al., 2016) were realized in 500 mL flasks with septa mounted on the stoppers. The flasks contained polymer samples (50 mg), topsoil [15 g, perlite (5.0 g) and mineral medium (10.8 mL)]. The flasks were incubated at 25°C. Head space gas was sampled at appropriate intervals through the septum with a gas-tight needle and conducted through a capillary into the gas analyzer (UAG, Stanford Instruments, USA) to determine the concentration of CO_2. The percentage of net mineralization with respect to the carbon content of the initial samples was calculated. Three parallel flasks were run for each sample, along with four blanks.

RESULTS AND DISCUSSION

Characterization of the Prepared Materials

Differential Scanning Calorimetry

Differential scanning calorimetry measurements of all samples reveal structure changes of PCL/TPS blends induced by blending with different TPS amounts (**Table 1**). The crystallinity (X_c) of the samples was calculated from the DSC curves recorded at the second heating ensuring the same thermal history of the samples. The DSC curves can be found in a **Supplementary File**.

With increasing amount of starch in the PCL/TPS blends T_m of PCL slightly decreased, which is in agreement with measurements of Averous et al. (2000). Rather negligible changes

TABLE 1 | Differential scanning calorimetry results for the PCL/TPS samples.

Physical quantities	PCL	PCL/TPS 70/30	PCL/TPS 50/50	PCL/TPS 30/70
T_m [°C]	57.3	56.7	56.7	55.8
T_c [°C]	30.8	30.2	28.2	26.7
ΔH_m [J·g^{-1}]	66.9	73.5	67.3	59.5
X_c [%]	49.6	54.5	49.9	44.1

in T_m partially within the experimental error of the measurement do not allow any conclusions regarding the PCL melting behavior changes induced by blending with TPS. No effect of the TPS on the PCL melting indicates immiscibility of PCL and thermoplastic starch. Contrary to this finding, Mittal et al. (2015) observed a significant decrease in T_m with increasing the TPS amount in the PCL/TPS blends, from which a partial miscibility or strong interactions between the components was deduced. A possible explanation of these contradictory findings in the literature can be seen in properties of thermoplastic starches used, which can differ significantly in composition (amylose/amylopectin ratio) and/or plasticizing system (type and amount of plasticizer). The proportion of PCL crystalline phase X_c increased after addition of 30% of TPS. This increase in matrix crystallinity in the presence of particles of minority phase is attributed to an enhanced nucleation at the interface (Sakai et al., 2009; Zhang et al., 2011). The enhanced nucleation by the interface can be further inferred from a decrease of T_c of PCL in PCL/TPS 50/50 and 30/70 blends. Although the crystallinity of the blend with 30 weight percent of TPS in comparison with the pure PCL slightly increased, the further increase in TPS content in the blends already led to the crystallinity decrease (PCL/TPS 50/50 and 30/70). In contrast to PCL/TPS (70/30) in the blend with 70% of TPS, the crystallinity is lower in comparison with the neat PCL. This blend has a co-continuous structure as it is shown in the following chapter with partially fine PCL domains. In such case geometrical constraints can suppress mobility of polymer chains and their crystallization. Since the DSC method is not sensitive enough for determination of glass transition in the case of semicrystalline polymers [often used for glass transition and crystallization temperature detection (Qiu et al., 2003)], the influence of adding different amount of TPS on changes of the glass transition of the final materials was not convincing. Therefore, these transitions were also analyzed by more sensitive DMTA method (see below **Figure 3** and **Table 2**).

Morphology Before Biodegradation

The micrographs in **Figure 1** display a representative morphology of the investigated samples before their composting or soil exposure. **Figures 1A,E** show a typical pure component morphology of the blend, i.e., PCL and wheat thermoplastic starch, respectively. Due to the plasticization procedure used, the TPS structure was almost homogeneous, in agreement with our previous work (Ostafinska et al., 2018). The other three micrographs, **Figures 1B–D**, demonstrate appropriate heterogeneous structure of the PCL/TPS blends. Polymer blend structure depends on many factors (processing conditions, ratio of blend components, etc.) and, thus, resulting morphology can vary. PCL/TPS 70/30 blend exhibits particle morphology of starch phase in PCL matrix (see **Figure 1B**). The size of TPS particles is typically in the range of few microns. Such a rather fine structure is in agreement with other studies on PCL/TPS blends found in the literature (Li and Favis, 2010; Huneault and Li, 2012) and suggests good compatibility between PCL and TPS. As pointed out by Huneault and Li (2012) and Koh et al. (2018), the compatibility in the TPS blends is influenced by the type and amount of plasticizing system, which affects both the viscosity of the TPS and the interactions between the blend components. A blend with 50 and 75% of TPS (see **Figures 1C,D**) shows morphology with irregular TPS domains. However, these starch domains are pronouncedly finer in a 50/50 blend (**Figure 1C**) than in the case of the PCL/TPS 30/70 blend (see **Figure 1D**). Although exact analysis of phase continuity was not performed, the structures observed are considered co-continuous, because by selective etching of both components, i.e., TPS by HCl and PCL by tetrahydrofuran (not shown) the specimens did not lose mechanical integrity. Formation of co-continuous structure in this blend is supported by distinctly lower viscosity of PCL in comparison with starch phase (see **Figure 2B**). Therefore, PCL, albeit a minority component, tends to form a continuous phase. Furthermore, Li and Favis (2010) proposed that a broad range of co-continuity in TPS blends can be explained by the high elasticity of the TPS component displaying gel-like behavior in the molten state (cf. **Figure 2A** and the discussion in the following section). On the one hand, a high elasticity prevents the deformation of molten particles in the flow; but on the other hand, once the particles are deformed, the elasticity hinders coalescence and/or retraction of irregular domains in the spherical shape and thus stabilizes the phase structure.

Rheological Characterization

The obtained rheological results clearly show relationship between specific concentration ratio of the blend components and the resulting rheological properties. Frequency sweeps of all analyzed samples at the temperature of 120°C are shown in **Figure 2**.

The frequency dependence of the storage modulus (**Figure 2A**) of the blends and the neat PCL and TPS plasticized by a two-step process exhibited a relatively large increase in the modulus of elasticity of more than 4 orders of magnitude with increasing TPS ratio in blend at an angular frequency of 0.1 rad/s. The blends containing 50% of TPS and more, which exhibit co-continuous phase structure (cf. **Figures 1C,D**), demonstrated gel-like behavior with nearly the same slope of the storage modulus curves. Since both the storage and loss modules ran in parallel, the corresponding damping factors ($\tan\delta = G''/G'$) were almost constant in the whole frequency range measured, except for the first point at the lowest angular frequency. Moreover, the damping factor of these blends is smaller than one, i.e., solid-like behavior dominates. On the contrary, the PCL/TPS 70/30 sample, i.e., the system with the smallest amount of starch

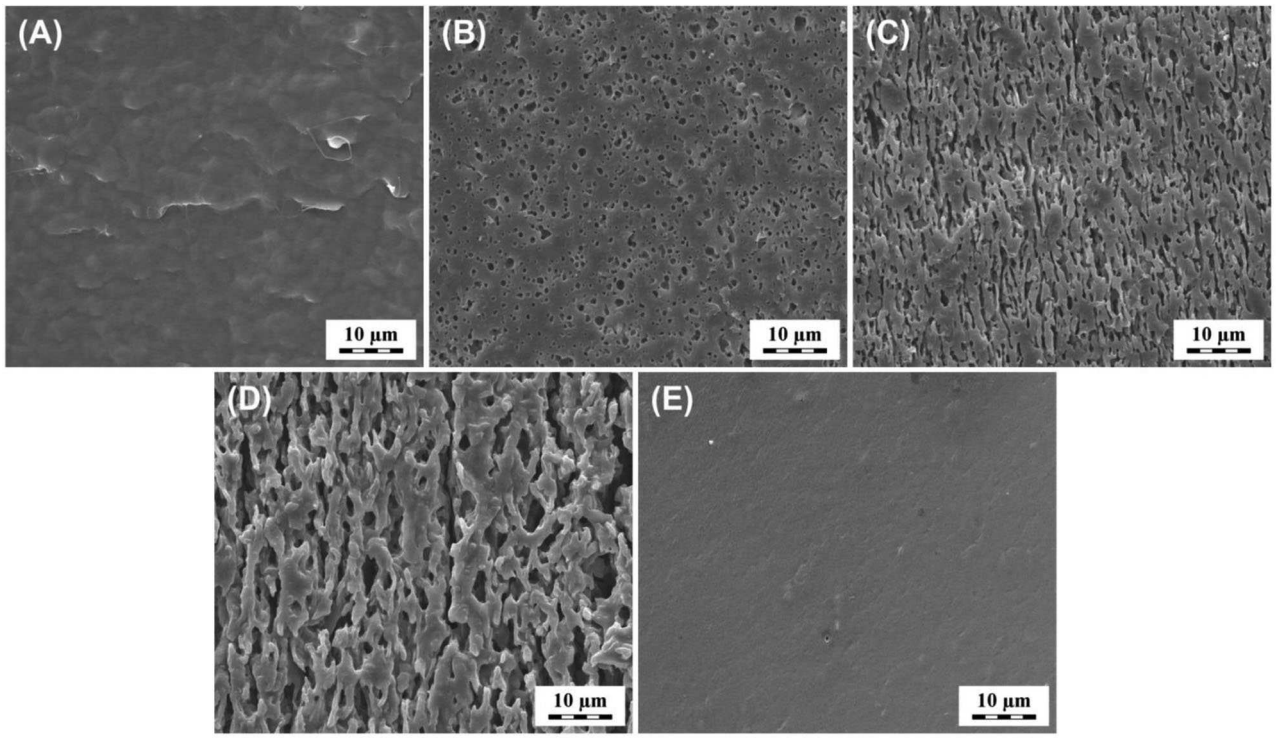

FIGURE 1 | SEM micrographs of smoothed pure components **(A)** PCL, **(E)** TPS and of smoothed etched surfaces of polymer blends, **(B)** PCL/TPS (70/30), **(C)** PCL/TPS (50/50), and **(D)** PCL/TPS (30/70) before biodegradation. Holes in the images correspond to TPS component of the blends etched off with 6 N HCl solution.

phase, showed a higher loss modulus than storage modulus values, meaning that the blend displayed behavior closer to pure PCL. PCL also demonstrated the lowest viscosity as expected (**Figure 2B**). Based on the recorded frequency dependencies of the complex viscosities of all melts (**Figure 2B**), the values have been increasing with increasing amount of TPS.

Dynamic Thermo-Mechanical Characterization

The thermo-mechanical behavior of the PCL/TPS blends, which was analyzed by dynamic mechanical thermal analysis, is shown in **Figure 3**. The thermodynamic results have provided information about the differences in flow behavior of the studied materials considering the weight ratio of blend components from the region below glass transition temperatures to their processing temperature. Thermal transitions, i.e., glass transitions of PCL- and TPS-phase of prepared materials, were determined from the maxima of the damping factor dependence on temperature.

The TPS displayed two glass transition temperatures corresponding to the glycerol-rich and starch-rich phases at −63 and 6.6°C, which is a typical feature of plasticized starch materials (Averous et al., 2000; Taguet et al., 2009; Li and Favis, 2010). The discussion of the thermal behavior of the PCL/TPS blends is complicated by the fact that the peaks of the glass transitions of the PCL and glycerol-rich TPS phases are overlapping (T_g of PCL was −58.1°C and T_g of glycerol-rich phase of TPS was −63°C). The PCL/TPS blends in this region 1 glass transition T_{g1} gradually decreasing with TPS content (**Table 2**). Therefore, it is hard to draw any strict conclusion about the miscibility of PCL and TPS from this shift. The glass transition temperature of the starch-rich phase T_{g2} in all the blends has been shifted from 6.6°C for neat TPS toward lower temperatures with increasing PCL content to −6.0°C for the PCL/TPS 70/30 blend (**Table 2**). In accordance with literature (Zhang et al., 2011), from this finding, strong molecular interactions based on hydrogen bonds between the carbonyl groups of PCL and hydroxyl groups of thermoplastic starch could be inferred (Matzinos et al., 2002; Rodriguez-Gonzalez et al., 2004). In the specific case of PCL and TPS, the situation is even more complicated, because PCL is soluble in glycerol, used as a plasticizer for TPS, at the processing temperature of 120°C. Moreover, phase separation in the TPS phase after blending leading to formation of a glycerol-rich layer at the interface is reported in the literature (Taguet et al., 2009; Koh et al., 2018). Thus, redistribution of glycerol between the PCL and TPS phases during melt mixing and subsequent cooling cannot be excluded.

All the blends demonstrated viscoelastic solid behavior in the whole temperature range, except for the blend with 30 wt. % of TPS, which changed to viscoelastic liquid at about 80°C. This change is characterized by the intersection of the G′ and G″ curves ($\tan \delta = 1$). Based on this result and in agreement with the frequency sweeps data (**Figure 2**), it could be concluded that in the PCL/TPS 70/30 blend, the PCL-phase has a dominant effect on the final rheological properties. Among all sample types, this

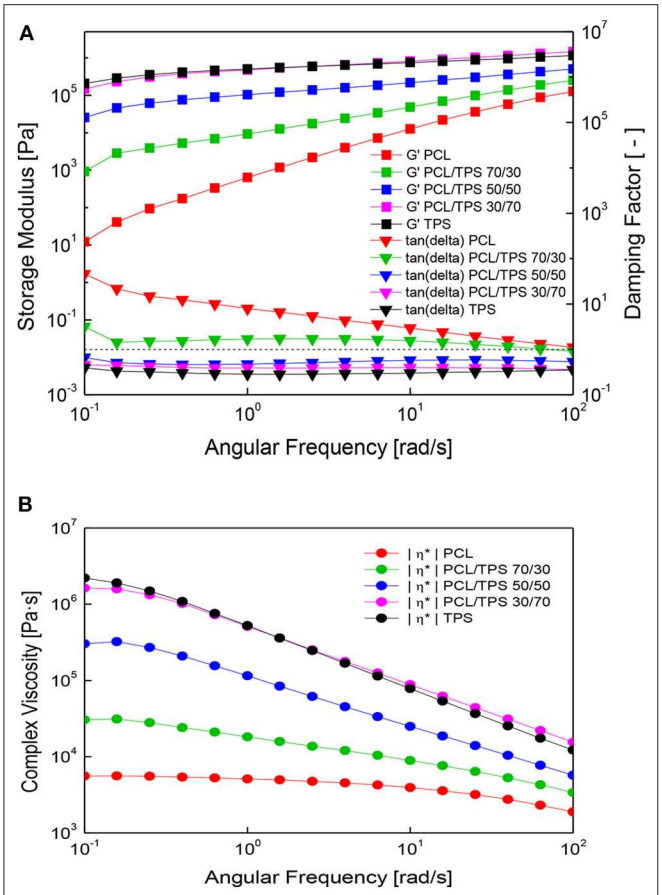

FIGURE 2 | Dependence of **(A)** storage modulus G' and damping factor tan δ, and **(B)** complex viscosity $|\eta^*|$ on the angular frequency ω of PCL/TPS-blends and their neat components ($T = 120°C$ and strain amplitude of 0.05%) (the dashed line shows tan $\delta = 1$).

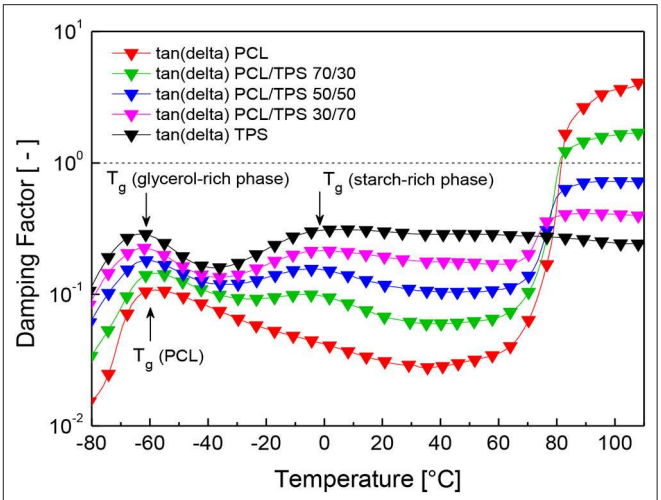

FIGURE 3 | Temperature dependence of damping factor tan δ of PCL/TPS blends and their pure components (the dashed line shows tan $\delta = 1$).

TABLE 2 | Glass transition temperatures (T_{g1} and T_{g2}) of the samples.

Temperature [°C]	PCL	PCL/TPS 70/30	PCL/TPS 50/50	PCL/TPS 30/70	TPS
T_{g1}	−58.1	−58.2	−59.6	−62.2	−63.0
T_{g2}		−6.0	−2.9	0.4	6.6

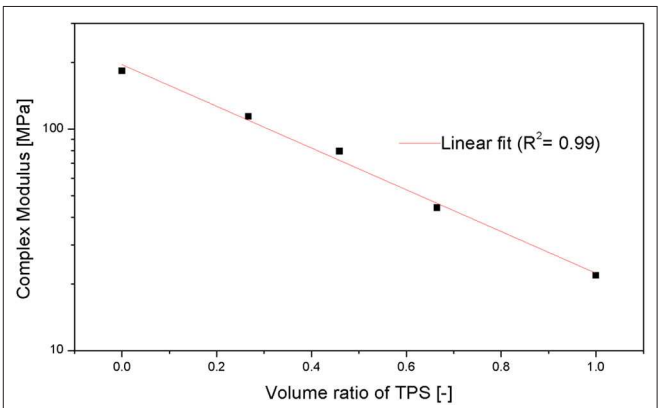

FIGURE 4 | Dependence and linear fit (red line) of the complex modulus absolute value $|G^*|$of PCL/TPS blends and their neat components on blend composition at frequency of 1 Hz, strain of 0.05% and temperature of 25°C.

blend and neat PCL showed behavior advantageous for example from the processing point of view.

For an evaluation of the compatibility of polymer blend components from rheological data logarithmic additivity rule is commonly used. This approach was adopted for complex modulus values at 25°C extracted from dynamic thermo-mechanical measurements. Fully immiscible blends usually show negative deviations from the additivity rule. As can be seen from **Figure 4**, the complex modulus follows the logarithmic additivity rule with a high accuracy. This agreement implies that the interfacial adhesion is high enough to ensure the stress transfer between phases and that PCL and TPS can be considered compatible.

Micro-Indentation Hardness Testing

Another tool for characterizing blend compatibility is the micro-indentation technique. The complete results of micro-indentation hardness testing measurements are summarized in **Table 3**.

The comparison of the micro-indentation results with predictive models is given in **Figure 5**.

To the first approximation, all the properties can be compared with the linear model (additivity law; dotted lines in **Figure 5**). The additivity law predicts that any final property of the system (P) is a linear combination of the properties of individual components:

$$P = \sum_i v_i P_i \tag{2}$$

where v_i and P_i are volume fractions and given properties of the individual components, respectively. The additivity law holds very well for polymer composites with infinitely long oriented fibers or for semicrystalline polymers (containing amorphous and crystalline phases). For most other polymer systems, however, the additivity law represents the upper achievable limit unless synergistic effects are observed (Ostafińska et al., 2017a; Ostafinska et al., 2018). In most cases, real mechanical properties are below the additivity law predictions due to the interface, which usually represents the weakest point. This was observed for all micromechanical properties in this work (E_{IT}, H_{IT}, C_{IT}, and η_{IT}–**Figures 5A–D**), but the negative deviations from additivity law were rather small, which indicated sufficient interfacial adhesion between the components (Šlouf et al., 2007). The strong interfacial adhesion, suggested by the behavior of E_{IT}, H_{IT}, C_{IT}, and η_{IT}, was consistent with other results in this study: (i) the non-etched fracture surfaces displayed no clear interface between the two phases, **Figure 1**, and (ii) dynamic thermo-mechanical measurements (**Figure 4**).

Moreover, the strong interfacial adhesion and good compatibility between TPS and PCL could be confirmed by the application of the equivalent box model (EBM; described in Kolařík, 1995, 1996), which could be applied to E_{IT} and H_{IT} (but not for C_{IT} and η_{IT}, which are beyond the EBM scope). Consequently, we could compare E_{IT} and H_{IT} experimental data with the theoretical EBM predictions:

$$E_b = E_1 v_{1p} + E_2 v_{2p} + \frac{v_s^2}{\left[\left(\frac{v_{1s}}{E_1}\right) + \left(\frac{v_{2s}}{E_2}\right)\right]} \quad (3)$$

$$H_b = H_1 v_{1p} + H_2 v_{2p} + A H_1 v_s \quad (4)$$

The details of the EBM model and the meaning of all its parameters were described elsewhere (Kolařík, 1996; Ostafińska et al., 2017a,b). Briefly, E_b and H_b represent the indentation modulus and hardness of the blend, E_i and H_i stand for the elastic modulus and the hardness of the individual components, and v_{ij} represents volume fractions of the components (the first subscript identifies the components and the second subscript

TABLE 3 | Results of micro-indentation hardness testing (the values present arithmetic mean and standard deviation from 30 independent measurements).

Code of sample	H_{IT} [MPa]	E_{IT} [GPa]	C_{IT} [%]	η_{IT} [%]
PCL	51.6 ± 1.6	0.68 ± 0.02	10.6 ± 0.3	43.4 ± 0.3
PCL/TPS 70/30	31.3 ± 1.2	0.50 ± 0.02	16.6 ± 0.5	33.8 ± 0.9
PCL/TPS 50/50	20.2 ± 0.9	0.42 ± 0.03	25.4 ± 0.9	25.3 ± 1.0
PCL/TPS 30/70	11.3 ± 0.6	0.37 ± 0.03	40.2 ± 1.1	14.7 ± 0.8
TPS	5.9 ± 0.5	0.24 ± 0.05	65.6 ± 3.2	10.1 ± 1.1

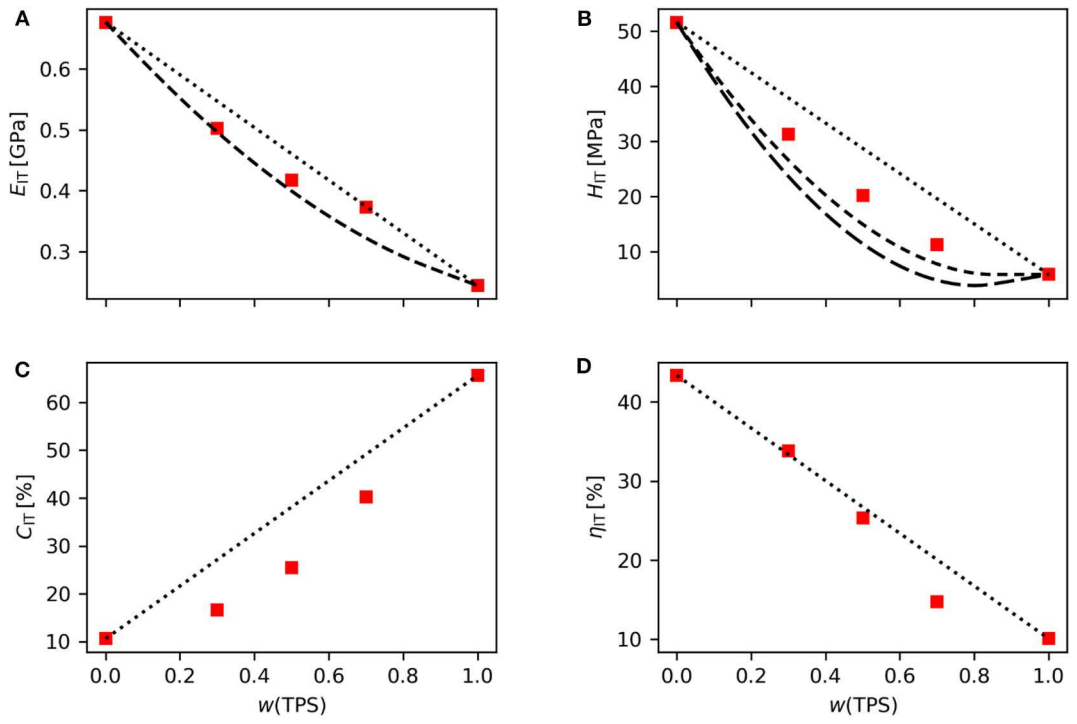

FIGURE 5 | Comparison of experimentally determined micromechanical properties (E_{IT}, H_{IT}, C_{IT}, and η_{IT}) with predictive models (dotted line = linear model/additive law, and dashed lines = EBM model). The linear model is applicable to all properties **(A–D)**; EBM theory has been developed and verified only for E_{IT} **(A)** and H_{IT} **(B)**. In case of H_{IT}, **(B)** the EBM prediction was calculated for both perfect interfacial adhesion (Equation 4 with A = 1; short dashed line) and for zero interfacial adhesion (according to Equation 4 with A = 0; long dashed line).

determines the volume of the component in parallel and serial branch of the EBM model, which correspond to the volume fractions with continuous and particulate morphology, respectively). The continuity of the components (i.e., the volume fractions v_{ij}) can be determined experimentally or estimated from percolation theory that predicts that continuity of the minority component starts at critical volume fraction $v_{cr} = 0.156$. Although the default, percolation theory-based value of the critical volume fraction ($v_{cr} = 0.156$) may seem rather low, many previous studies documented that EBM predictions calculated with this default value were in very good agreement with experimental results (Kolařík, 1996; Vacková et al., 2012; Ostafinska et al., 2015; Ostafińska et al., 2017a,b). In order to understand v_{cr} parameter properly, it is also important to realize that it represents the composition at which a small fraction of minority phase may start to be continuous according to percolation theory, while most of this phase still exhibits particulate structure. This is more evident if we calculate all volume fractions v_{ij} (i.e., v_{1p}, v_{2p}, v_{1s}, and v_{2s} in Equations 3 and 4) as described elsewhere (Kolařík, 1996; Ostafinska et al., 2018). Therefore, default value of critical volume fraction may be regarded as a parameter, which (i) represents the theoretically predicted composition at which the first signs of co-continuity may appear and which (ii) corresponds reasonably well with experimental results if more detailed analysis of morphology for given system is not available (Kolařík, 1995, 1996, 2000). The last parameter A describes interfacial adhesion (the values $A = 0$ and 1 mean negligible and perfect adhesion, respectively). We performed the EBM calculations (based on default $v_{cr} = 0.156$) for both E_{IT} and H_{IT} (**Figure 5**, dashed lines). Moreover, for H_{IT}, the calculation was made for both minimal interfacial adhesion ($A = 0$; short dashed line) and maximal interfacial adhesion ($A = 1$; long dashed line). The fact that the experimental values of E_{IT} were higher than the EBM predictions (**Figure 5A**) indicated good compatibility and strong interface between PCL and TPS (Kolařík, 2000; Vacková et al., 2012; Ostafinska et al., 2018). The good PCL/TPS compatibility was confirmed also by the experimental values of H_{IT} (**Figure 5B**) which corresponded better to the EBM prediction based on maximal interfacial adhesion (**Figure 5B**, short dashed line corresponding to Equation 4 with $A = 1$) than to the EBM prediction based on minimal interfacial adhesion (**Figure 5B**, long dashed line corresponding to Equation 4 with $A = 0$). If the blends had been incompatible (i.e., if the interfacial adhesion was negligible and $A = 0$), the experimental values of $H_{IT} \approx Y$ would have shown a local minimum as documented elsewhere (Kolařík, 1995; Šlouf et al., 2007). Furthermore, the good interfacial adhesion in our PCL/TPS systems was indicated not only by the micro-indentation experiments described in this section, but also by rheological measurements described in the previous section (see **Figure 4** and its discussion above).

The applicability of the EBM model to micromechanical properties has been justified theoretically and verified experimentally in our previous studies (Ostafinska et al., 2015; Ostafińska et al., 2017a,b; Ostafinska et al., 2018). We conclude that all micromechanical properties (E_{IT}, H_{IT}, C_{IT} and η_{IT}) were close to the linear model predictions and two micromechanical properties (E_{IT} and H_{IT}) were higher than the EBM model predictions, which could be attributed to the very good compatibility and strong interfacial adhesion between the blend components.

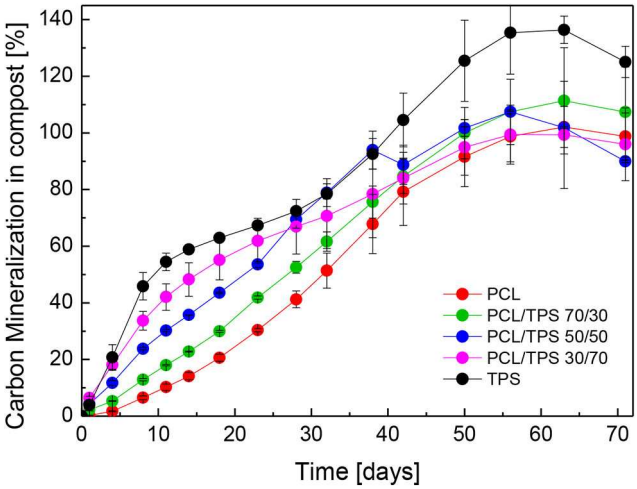

FIGURE 6 | Biodegradation rate of PCL/TPS blends and their pure components under the composting conditions.

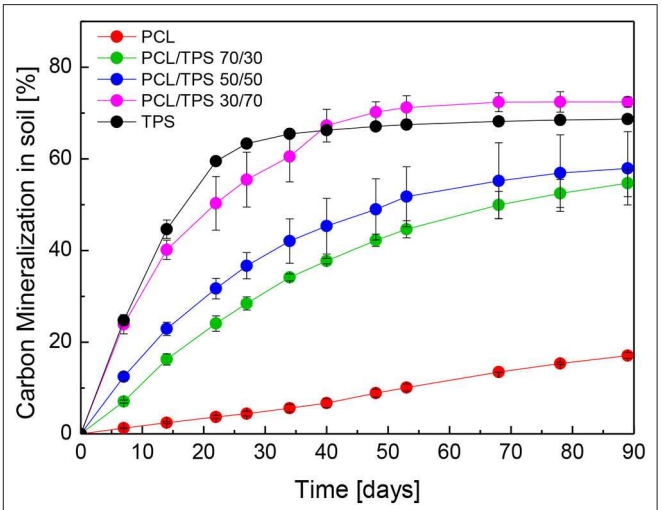

FIGURE 7 | Biodegradation rate of PCL/TPS blends and their pure components in soil conditions ($T = 25°C$).

Biodegradation

Biodegradation Under Composting Conditions

The conditions of industrial composting are characterized by the temperature of 58°C, which is already in the melting temperature region of PCL. Consequently, the crystalline parts of PCL do not represent an obstacle for enzymes and the biodegradation of all the materials was relatively rapid (see **Figure 6**). However, still the initial rate of biodegradation reflected the content of the easily biodegradable starch. In PCL/TPS 30/70, the curve even followed

the initial fast phase, which probably witnesses the build-up of the microbial biomass. In the later phase of the biodegradation the materials with higher PCL contents, even pure PCL, aligned with the other materials and reached the total biodegradation almost simultaneously. Thus, all the PCL based blend materials were well compatible with the composting as an eventual projected end-of-life solution. The biodegradation of several samples over 100% is not unusual especially in compost environment, which contains a large amount of organic carbon. The part of this carbon can be mobilized by the microorganisms induced with the sample addition.

Biodegradation in Soil Conditions

Very fast biodegradation of the neat TPS reached about 70% mineralization at the end of the experiment (see **Figure 7**). It is not unusual that a fast degrading material does not reach a higher level of mineralization because an important part of the carbon is bound in the biomass and subsequently released on a much slower rate. ISO 17556 (2012) expects validity of the test at a minimal 60% mineralization of an easily degradable reference material. Biodegradation in soil was governed by the PCL content in the materials. As mentioned in the introduction, soil biodegradation of the different PCL grades can differ

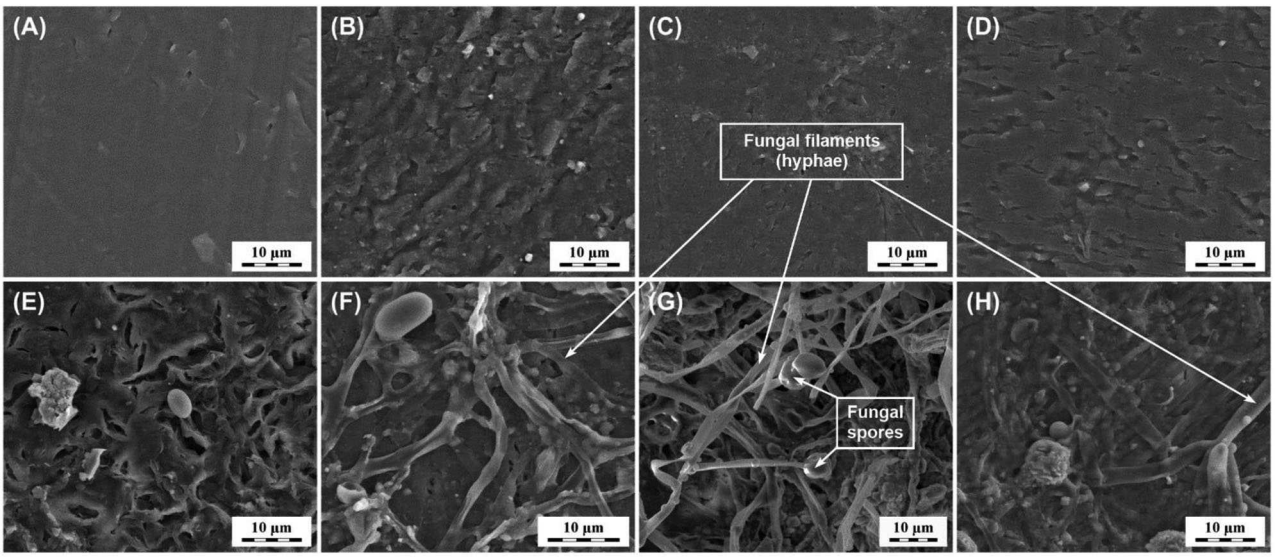

FIGURE 8 | SEM micrographs of sample surface: **(A)** PCL, **(B)** PCL/TPS 70/30, **(C)** PCL/TPS 50/50, **(D)** PCL/TPS 30/70 before biodegradation and **(E)** PCL, **(F)** PCL/TPS 70/30, **(G)** PCL/TPS 50/50, **(H)** PCL/TPS 30/70 after 20 days of biodegradation in soil.

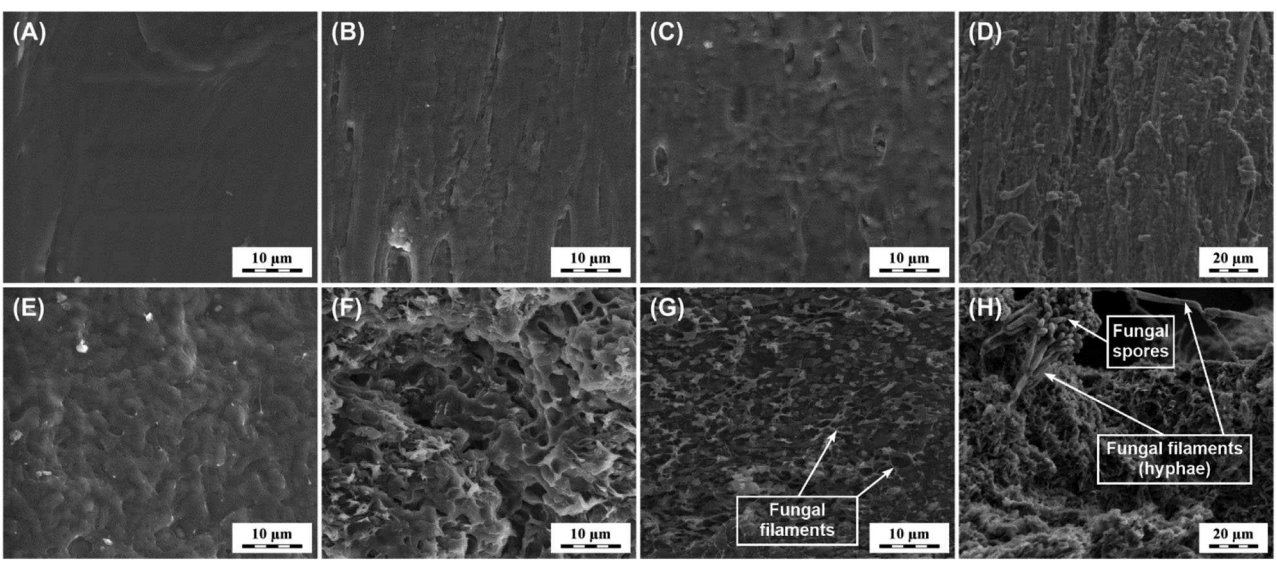

FIGURE 9 | SEM micrographs of fracture surfaces: **(A)** PCL, **(B)** PCL/TPS 70/30, **(C)** PCL/TPS 50/50, **(D)** PCL/TPS 30/70 before biodegradation and **(E)** PCL, **(F)** PCL/TPS 70/30, **(G)** PCL/TPS 50/50, **(H)** PCL/TPS 30/70 after 20 days of biodegradation in soil.

considerably, depending mainly on the molecular weight of the polymer and the crystallinity of the resulting material. Here, relatively high molecular weight PCL was used, so it could be expected that the biodegradation of PCL and the PCL phase in the blends could be retarded. The initial rate of the biodegradation clearly reflected the morphology of the materials. The PCL/TPS 30/70, in which the starch forms a continuous phase, decomposed at the initial rate almost identical to the neat TPS. In contrast, the PCL/TPS 50/50 and the PCL/TPS 70/30 were initially mineralized at much slower rate, probably because the continuous PCL phase restricted to some extent the availability of TPS to the enzymes. It was not clearly evident whether the TPS content was able to accelerate the biodegradation of the PCL phase, on the other hand, the PCL content was successfully used to retard the biodegradation of the TPS phase, which could be useful in certain applications where the material comes into contact with microorganisms and must retain its properties for a given time.

Morphology Characterization After Biodegradation

Morphological changes in the materials during the biodegradation process in soil and the microbial colonization of samples were observed by SEM. SEM micrographs of the samples surfaces before and after 20 days of incubation in soil at 25°C are shown in **Figure 8**. The initial samples showed a smooth surface in the case of the neat PCL (**Figure 8A**) and morphological structures of the PCL/TPS samples reflecting the pattern of domains of PCL and TPS (**Figures 8B–D**). The surface of the PCL/TPS 50/50 sample (**Figure 8C**) seems to be smoother than the surfaces of blends with majority phases of PCL and TPS, respectively (**Figures 8B,D**). After the indicated period of biodegradation, neat PCL exhibited surface cracks but only scarcely present microorganisms (**Figure 8E**). On the contrary TPS containing samples are covered with biofilm consisting mainly of fungal hyphae and fungal spores (**Figures 8F–H**). It could be estimated that the density of the biofilm is increasing with the TPS content in samples.

The similar situation could be seen on the pictures showing the fracture surfaces of the samples (**Figure 9**). From the micrographs of blends before biodegradation (**Figures 9A–D**) it is hard to distinguish individual phases, probably because the fracture path does not follow the interface preferentially. This can be taken as another hint of good interfacial adhesion between PCL and TPS together with findings from rheological and mechanical measurements discussed before. Initial sample morphologies again reflected the blending of the components whereas this time the PCL/TPS 30/70, the PCL/TPS 70/30, and the PCL/TPS 30/70 (**Figures 9B,D**) were different with much higher apparent inhomogeneity in the PCL/TPS 30/70 sample (**Figure 9D**). After the biodegradation, the structural degradation

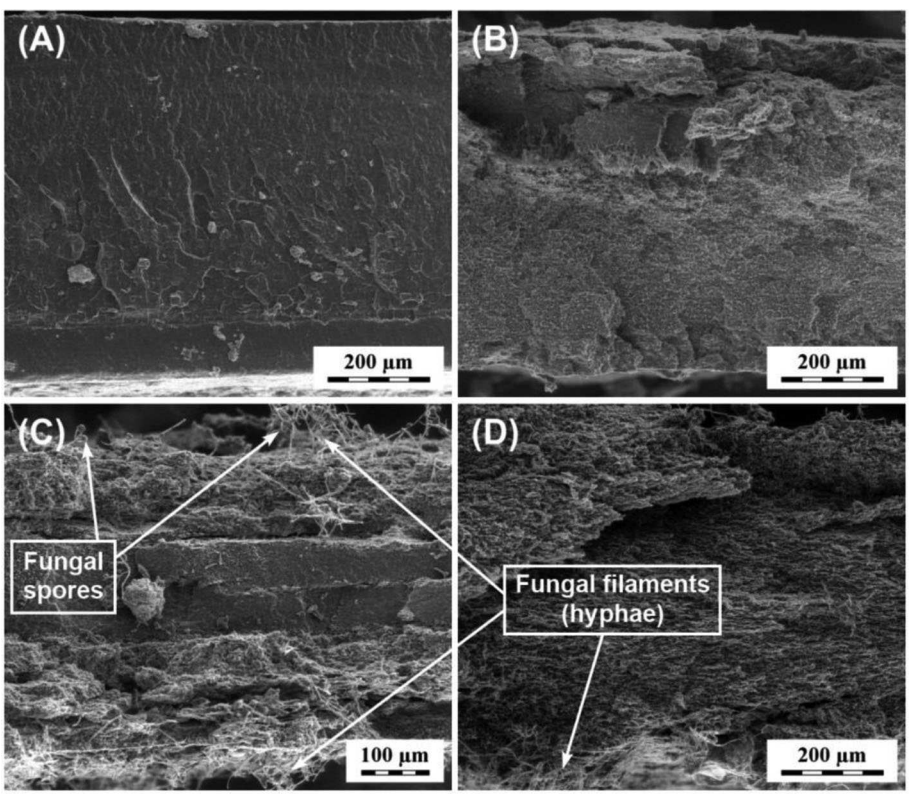

FIGURE 10 | SEM micrographs of fracture surfaces with lower magnification showing the whole profile of the sample films: **(A)** PCL, **(B)** PCL/TPS 70/30, **(C)** PCL/TPS 50/50, **(D)** PCL/TPS 30/70 after 20 days of biodegradation in soil.

of the sample was clearly a function of the TPS content, where the voids in the structure most probably were a consequence of the starch degradation and disappearance. These voids were colonized with microorganisms. These were not apparent in the PCL and PCL/TPS 70/30 samples (**Figure 9F**) but could be seen as thin bacterial filaments, probably actinomycetes, in the PCL/TPS 50/50 sample (**Figure 9G**), and also as much thicker fungal filaments and conidia in the PCL/TPS 30/70 sample (**Figure 9H**).

The pictures of the fractured specimens made at a lower magnification (**Figure 10**) showing the whole thickness of the samples clearly illustrate the biodegradation progress from the specimen surface to its center. The PCL and PCL/TPS 70/30 samples are eroded in the thin surface layer only, while the PCL/TPS 50/50 sample (**Figure 10C**) exhibited deep erosion and penetration of the fungal hyphae and only a central layer comprising about one third of the material thickness stayed relatively unaffected. The PCL/TPS 30/70 sample (**Figure 10D**) was then completely eroded in the whole its thickness.

The pattern of morphological changes during biodegradation suggests the importance of organization of the blend phases. Whereas, the easily biodegradable TPS phase inclusions are surrounded and isolated by the continuous PCL phase in the PCL/TPS 70/30 material (**Figure 1**) in the PCL/TPS 50/50 and PCL/TPS 30/70 materials, TPS creates a continuous phase of interconnected domains, which greatly facilitate the penetration of enzymes and microorganisms and as a consequence the erosion and biodegradation of the material.

CONCLUSION

The present article has demonstrated that the morphology of the PCL/TPS blends and their resulting properties, particularly their biodegradability, can be controlled by the composition of their components.

The PCL/TPS blends investigated were characterized in detail by rheological, thermomechanical, and micromechanical measurements. The results of these examinations showed that there are interactions between PCL and TPS and that these polymers form compatible polymer blends with good interfacial adhesion.

The measurements showed that the addition of thermoplastic starch has a negligible effect on the final crystallization of PCL in the blends. Thus, our results indicate that the PCL crystallinity is not a dominant parameter determining the biodegradation rate, as has often been declared in the literature.

From our findings, a correlation between the biodegradation course of the samples and the size of the interfacial area can be inferred. It significantly changes due to the ratio of PCL/TPS blend components. Nevertheless, according to our results and in agreement with the literature, the interactions and the structure formation are rather complex in these blends, because the TPS plasticizer is miscible with PCL at processing temperatures and, thus, the interpretation of the findings and predictions regarding the final properties are difficult.

The composting conditions were characterized by the temperature, which is already in the melting temperature region of PCL. Thus, the crystalline parts of PCL did not represent an obstacle for enzymes and the biodegradation of all the materials was relatively rapid. Biodegradation in soil brought out more remarkable differences between blends with different TPS content. Biodegradation evaluation of the PCL/TPS samples in the soil environment revealed that firstly, voids in the samples appeared due to faster TPS biodegradation and were then colonized by microorganisms. These were not apparent in the neat PCL and PCL/TPS 70/30 blend but could be clearly distinguished in the PCL/TPS 50/50 as thin bacterial filaments and as much thicker fungal filaments and conidia in the case of PCL blended with 70 wt. % of plasticized starch. The initial rate of biodegradation increased with the content of easily biodegradable starch in the sample. The materials with higher PCL contents were initially mineralized at much slower rate because the continuous PCL phase successfully restricted the availability of TPS for enzymes. The key role of the phase structure for the biodegradation course was further confirmed by morphological analysis of the samples after biodegradation.

The findings obtained from the study presented in this paper show that controlling phase structure by blends composition enables one to tailor the biodegradation rate of the PCL/TPS blends. Following from that, the results are applicable in production of environmental-friendly materials.

DATA AVAILABILITY STATEMENT

All datasets generated for this study are included in the article/**Supplementary Material**.

AUTHOR CONTRIBUTIONS

MN and MK designed the study. AU prepared the samples. SEM sample visualization was done by MN and AU. MN performed the DSC, rheology, and DMTA measurements and together with ZS, ZK, and IF evaluated and made the final interpretation of the results. HV carried out the micro-indentation hardness testing and MŠ processed and evaluated these data. JŠ performed all the biodegradation measurement and MK explicated the collected biodegradation data. MN, MK, and ZS prepared the draft of the manuscript, which was finalized in cooperation with all co-authors.

ACKNOWLEDGMENTS

Financial support through grant NV15-31269A (MH CR) was gratefully acknowledged. Electron microscopy at the Institute of Macromolecular Chemistry was supported by projects TE01020118, TN01000008, and (Technology Agency of the CR) and POLYMAT LO1507 (Ministry of Education, Youth and Sports of the CR, program NPU I).

SUPPLEMENTARY MATERIAL

The Supplementary Material for this article can be found online at: https://www.frontiersin.org/articles/10.3389/fmats.2020.00141/full#supplementary-material

REFERENCES

Albertsson, A.-C., and Varma, I. K. (2002). "Aliphatic polyesters: synthesis, properties and applications," in *Degradable Aliphatic Polyesters I*, eds. G. Scott and D. Gileat (London: Springer), 1–40. doi: 10.1007/3-540-45734-8_1

Avérous, L. (2004). Biodegradable multiphase systems based on plasticized starch: a review. *J. Macromol. Sci. Polym. Rev*. 44, 231–274. doi: 10.1081/MC-200029326

Averous, L., Moro, L., Dole, P., and Fringant (2000). Properties of thermoplastic blends: starch-polycaprolactone. *Polymer*. 41, 4157–4167. doi: 10.1016/S0032-3861(99)00636-9

Bastioli, C. (1998). Biodegradable materials–present situation and future perspectives. *Macromol. Symp*. 135, 193–204. doi: 10.1002/masy.19981350122

Campos, A., de Marconato, J. C., and Martins-Franchetti, S. M. (2012). The influence of soil and landfill leachate microorganisms in the degradation of PVC/PCL films cast from DMF. *Polímeros* 22, 220–227. doi: 10.1590/S0104-14282012005000029

Cesur, S. (2018). The effects of additives on the biodegradation of polycaprolactone composites. *J. Polym. Environ*. 26, 1425–1444. doi: 10.1007/s10924-017-1029-y

Chang, H.-M. M., Huang, C.-C. C., Parasuraman, V. R., Jhu, J.-J. J., Tsai, C.-Y. Y., Chao, H.-Y. Y., et al. (2017). *In vivo* degradation of poly (ε-caprolactone) films in gastro intestinal (GI) tract. *Mater. Today Commun.* 11, 18–25. doi: 10.1016/j.mtcomm.2017.01.006

Dřímal, P., Hoffmann, J., and Družbík, M. (2007). Evaluating the aerobic biodegradability of plastics in soil environments through GC and IR analysis of gaseous phase. *Polym. Test*. 26, 729–741. doi: 10.1016/j.polymertesting.2007.03.008

Düskünkorur, H. (2012). *Biopolyester Synthesis by Enzymatic Catalysis and Development of Nanohybrid Systems*. Available online at: https://tel.archives-ouvertes.fr/tel-00864276

Fortelný, I., Lapčíková, M., Lednický, F., Starý, Z., and Kruliš, Z. (2008). Nonuniformity of phase structure in immiscible polymer blends. *Polym. Eng. Sci*. 48, 564–571. doi: 10.1002/pen.20985

Funabashi, M., Ninomiya, F., and Kunioka, M. (2009). Biodegradability Evaluation of Polymers by ISO 14855-2. *Int. J. Mol. Sci*. 10, 3635–3654. doi: 10.3390/ijms10083635

Herrman, K. (Ed.). (2011). *Hardness Testing: Principles and Applications*. Novelty, OH: ASM International.

Horák, Z., Fortelný, I., Kolařík, J., Hlavatá, D., and Sikora, A. (2005). "Polymer blends," in *Encyclopedia of Polymer Science and Technology* (John Wiley & Sons), 1–59. doi: 10.1002/0471440264.pst276

Huneault, M. A., and Li, H. (2012). Preparation and properties of extruded thermoplastic starch/polymer blends. *J. Appl. Polym. Sci*. 126, E96–E108. doi: 10.1002/app.36724

Imre, B., and Pukánszky, B. (2013). Compatibilization in bio-based and biodegradable polymer blends. *Eur. Polym. J*. 49, 1215–1233. doi: 10.1016/j.eurpolymj.2013.01.019

Innocenti, F. D. (2005). "Biodegradation behaviour of polymers in the soil," in *Handbook of Biodegradable Polymers*, ed C. Bastioli (Shrewsbury: Rapra Technology Limited), 57–102.

Iwamoto, A., and Tokiwa, Y. (1994). Effect of the phase structure on biodegradability of polypropylene/poly(ε-caprolactone) blends. *J. Appl. Polym. Sci*. 52, 1357–1360. doi: 10.1002/app.1994.070520920

Jayasekara, R., Harding, I., Bowater, I., and Lonergan, G. (2005). Biodegradability of a selected range of polymers and polymer blends and standard methods for assessment of biodegradation. *J. Polym. Environ*. 13, 231–251. doi: 10.1007/s10924-005-4758-2

Khatiwala, V. K., Shekhar, N., Aggarwal, S., and Mandal, U. K. (2008). Biodegradation of poly(ε-caprolactone) (pcl) film by alcaligenes faecalis. *J. Polym. Environ*. 16, 61–67. doi: 10.1007/s10924-008-0104-9

Koh, J. J., Zhang, X., and He, C. (2018). Fully biodegradable poly(lactic acid)/starch blends: a review of toughening strategies. *Int. J. Biol. Macromol.* 109, 99–113. doi: 10.1016/j.ijbiomac.2017.12.048

Kolařík, J. (1995). Prediction of the yield strength of polymer blends. *Polym. Netw. Blends* 5, 87–93.

Kolařík, J. (1996). Simultaneous prediction of the modulus and yield strength of binary polymer blends. *Polym. Eng. Sci*. 36, 2518–2524. doi: 10.1002/pen.10650

Kolařík, J. (2000). Positive deviations of the modulus and yield strength of blends consisting of partially miscible polymers. *J. Macromol. Sci. B*39, 53–66. doi: 10.1081/MB-100100371

Labet, M., and Thielemans, W. (2009). Synthesis of polycaprolactone: a review. *Chem. Soc. Rev*. 38, 3484. doi: 10.1039/b820162p

Leja, K., and Lewandowicz, G. (2010). Polymer biodegradation and biodegradable polymers. *Polish J. Environ. Stud.* 19, 255–266.

Li, G., and Favis, B. D. (2010). Morphology development and interfacial interactions in polycaprolactone/thermoplastic-starch blends. *Macromol. Chem. Phys*. 211, 321–333. doi: 10.1002/macp.200900348

Matzinos, P., Tserki, V., Kontoyiannis, A., and Panayiotou, C. (2002). Processing and characterization of starch/polycaprolactone products. *Polym. Degrad. Stab*. 77, 17–24. doi: 10.1016/S0141-3910(02)00072-1

Mittal, V., Akhtar, T., and Matsko, N. (2015). Mechanical, thermal, rheological and morphological properties of binary and ternary blends of PLA, TPS and PCL. *Macromol. Mater. Eng*. 300, 423–435. doi: 10.1002/mame.201400332

Mudhoo, A., Mohee, R., Unmar, G. D., and Sharma, S. K. (2011). "Degradation of biodegradable and green polymers in the composting environment," in *A Handbook of Applied Biopolymer Technology: Synthesis, Degradation and Applications*, eds S. K. Sharma and A. Mudhoo (Cambridge: RSC), 332–364.

Nagata, M., and Yamamoto, Y. (2009). Synthesis and characterization of photocrosslinked poly(ε-caprolactone)s showing shape-memory properties. *J. Polym. Sci. Part A Polym. Chem*. 47, 2422–2433. doi: 10.1002/pola.23333

Narancic, T., Verstichel, S., Chaganti, S. R., Morales-Gamez, L., Kenny, S. T., Wilde, B., et al. (2018). Biodegradable plastic blends create new possibilities for end-of-life management of plastics but they are not a panacea for plastic pollution. *Environ. Sci. Technol*. 52, 10441–10452. doi: 10.1021/acs.est.8b02963

Nevoralová, M., Ujčić, A., Kodakkadan, Y. N. V., and Starý, Z. (2019). Rheological characterization of starch-based biodegradable polymer blends. *AIP Conf. Proc.* 2017:050005. doi: 10.1063/1.5109511

Oliver, W. C., and Pharr, G. M. (1992). An improved technique for determining hardness and elastic modulus using load and displacement sensing indentation experiments. *J. Mater. Res*. 7, 1564–1583. doi: 10.1557/JMR.1992.1564

Ostafińska, A., Fortelný, I., Hodan, J., Krejčíková, S., Nevoralová, M., Kredatusová, J., et al. (2017a). Strong synergistic effects in PLA/PCL blends: impact of PLA matrix viscosity. *J. Mech. Behav. Biomed. Mater*. 69, 229–241. doi: 10.1016/j.jmbbm.2017.01.015

Ostafinska, A., Fortelny, I., Nevoralova, M., Hodan, J., Kredatusova, J., and Slouf, M. (2015). Synergistic effects in mechanical properties of PLA/PCL blends with optimized composition, processing, and morphology. *RSC Adv*. 5, 98971–98982. doi: 10.1039/C5RA21178F

Ostafińska, A., Mikešová, J., Krejčíková, S., Nevoralová, M., Šturcová, A., Zhigunov, A., et al. (2017b). Thermoplastic starch composites with TiO_2 particles: preparation, morphology, rheology and mechanical properties. *Int. J. Biol. Macromol.* 101, 273–282. doi: 10.1016/j.ijbiomac.2017.03.104

Ostafinska, A., Vackova, T., and Slouf, M. (2018). Strong synergistic improvement of mechanical properties in HDPE/COC blends with fibrillar morphology. *Polym. Eng. Sci*. 58, 1955–1964. doi: 10.1002/pen.24805

Parulekar, Y., and Mohanty, A. K. (2007). Extruded biodegradable cast films from polyhydroxyalkanoate and thermoplastic starch blends: fabrication and characterization. *Macromol. Mater. Eng*. 292, 1218–1228. doi: 10.1002/mame.200700125

Potts, J. E. E., Clendinning, R. A. A., Ackart, W. B. B., and Niegisch, W. D. D. (1973). "The biodegradability of synthetic polymers," in *Polymer Science and Technologyolymers and Ecological Problems*, ed J. Guillet (New York, NY: Plenum Press), 61–79. doi: 10.1007/978-1-4684-0871-3_4

Qiu, Z., Ikehara, T., and Nishi, T. (2003). Poly(hydroxybutyrate)/poly(butylene succinate) blends: miscibility andnonisothermal crystallization. *Polymers* 44, 2503–2508. doi: 10.1016/S0032-3861(03)00150-2

Rochman, C. M., Browne, M. A., Halpern, B. S., Hentschel, B. T., Hoh, E., Karapanagioti, H. K., et al. (2013). Classify plastic waste as hazardous. *Nature* 494, 169–171. doi: 10.1038/494169a

Rodriguez-Gonzalez, F. J., Ramsay, B. A., and Favis, B. D. (2004). Rheological and thermal properties of thermoplastic starch with high glycerol content. *Carbohydr. Polym*. 58, 139–147. doi: 10.1016/j.carbpol.2004.06.002

Rudnik, E. (2013). "Compostable polymer properties and packaging applications," in *Plastic Films in Food Packaging,* ed S. Ebnesajjad (Waltham, MA: Elsevier), 217–248. doi: 10.1016/B978-1-4557-3112-1.00013-2

Rutkowska, M., Krasowska, K., Heimowska, A., Steinka, I., Janik, H., Haponiuk, J., et al. (2002). Biodegradation of modified poly(ε-caprolactone) in different environments. *Polish J. Environ. Stud*. 11, 413–420.

Sakai, F., Nishikawa, K., Inoue, Y., and Yazawa, K. (2009). Nucleation enhancement effect in poly(L-lactide) (PLLA)/poly(ϵ-caprolactone) (PCL) blend induced by locally activated chain mobility resulting from limited miscibility. *Macromolecules* 42, 8335–8342. doi: 10.1021/ma901547a

Sanchez, J. G., Tsuchii, A., and Tokiwa, Y. (2000). Degradation of polycaprolactone at 50°C by a thermotolerant aspergillus sp. *Biotechnol. Lett*. 22, 849–853. doi: 10.1023/A:1005603112688

Sessini, V., Arrieta, M. P., Fernández-Torres, A., and Peponi, L. (2018). Humidity-activated shape memory effect on plasticized starch-based biomaterials. *Carbohydr. Polym*. 179, 93–99. doi: 10.1016/j.carbpol.2017.09.070

Shaw, M. T. (1985). "Microscopy and other methods of studying blends," in *Polymer Blends and Mixtures*, eds D. J. Walsh, J. S. Higgins, and A. Maconnachie (Dordrecht: Springer), 480. doi: 10.1007/978-94-009-5101-3_3

Singh, R., P., Pandey, J. K., Rutot, D., Degée, P., and Dubois, P. (2003). Biodegradation of poly(ε-caprolactone)/starch blends and composites in composting and culture environments: The effect of compatibilization on the inherent biodegradability of the host polymer. *Carbohydr. Res*. 338, 1759–1769. doi: 10.1016/S0008-6215(03)00236-2

Šlouf, M., Kolařík, J., and Kotek, J. (2007). Rubber-toughened polypropylene/acrylonitrile-co-butadiene-co-styrene blends: Morphology and mechanical properties. *Polym. Eng. Sci*. 47, 582–592. doi: 10.1002/pen.20727

Slouf, M., Pavlova, E., Krejcikova, S., Ostafinska, A., Zhigunov, A., Krzyzanek, V., et al. (2018). Relations between morphology and micromechanical properties of alpha, beta and gamma phases of iPP. *Polym. Test*. 67, 522–532. doi: 10.1016/j.polymertesting.2018.03.039

Stloukal, P., Jandikova, G., Koutny, M., and Sedlarík, V. (2016). Carbodiimide additive to control hydrolytic stability and biodegradability of PLA. *Polym. Test*. 54, 19–28. doi: 10.1016/j.polymertesting.2016.06.007

Swain, S. N., Biswal, S. M., Nanda, P. K., and Nayak, P. L. (2004). Biodegradable soy-based plastics: opportunities andchallenges. *J. Polym. Environ*. 12, 35–42. doi: 10.1023/B:JOOE.0000003126.14448.04

Taguet, A., Huneault, M. A., and Favis, B. D. (2009). Interface/morphology relationships in polymer blends with thermoplastic starch. *Polymers* 50, 5733–5743. doi: 10.1016/j.polymer.2009.09.055

Vacková, T., Slouf, M., Nevoralová, M., and Kaprálková, L. (2012). HDPE/COC blends with fibrous morphology and their properties. *Eur. Polym. J*. 48, 2031–2039. doi: 10.1016/j.eurpolymj.2012.09.005

Vikman, M., Hulleman, S. H. D., Van Der Zee, M., Myllarinen, P., and Feil, H. (1999). Morphology and enzymatic degradation of thermoplastic starch-polycaprolactone blends. *J. Appl. Polym. Sci*. 74, 2594–2604. doi: 10.1002/(SICI)1097-4628(19991209)74:11<2594::AID-APP5>3.0.CO;2-R

Villar, M. A., Barbosa, S. E., García, M. A., Castillo, L. A., and López, O. V. (2017). "Starch-based materials in food packaging," in *Processing, Characterization and Aplications*, eds A. M. Villar, S. E. Barbosa, and O. V. López (Cambridge: Elsevier; Academic Press), 336.

Vroman, I., Tighzert, L., Vroman, I., and Tighzert, L. (2009). Biodegradable polymers. *Materials* 2, 307–344. doi: 10.3390/ma2020307

Wang, X.-L., Yang, K.-K., and Wang, Y.-Z. (2003). Properties of starch blends with biodegradable polymers. *J. Macromol. Sci. Part C Polym*. 43, 385–409. doi: 10.1081/MC-120023911

Wang, X. J., Gross, R. A., and McCarthy, S. P. (1995). Rheological study of biodegradable blends of starch and polyvinyl alcohol. *J. Environ. Polym. Degrad*. 3, 161–167. doi: 10.1007/BF02068467

Zhang, K., Ran, X., Wang, X., Han, C., Han, L., Al., et al. (2011). Improvement in toughness and crystallization of poly(l-lactic acid) by melt blending with poly(epichlorohydrin-co-ethylene oxide). *Polym. Eng. Sci*. 51, 2370–2380. doi: 10.1002/pen.22009

Conflict of Interest: The authors declare that the research was conducted in the absence of any commercial or financial relationships that could be construed as a potential conflict of interest.